

Photo-Cross-Linked Single-Ion Conducting Polymer Electrolyte for Lithium-Metal Batteries

Hai-Peng Liang, Zhen Chen, Xu Dong, Tatiana Zinkevich, Sylvio Indris, Stefano Passerini,* and Dominic Bresser*

Polymer electrolytes are considered potential key enablers for lithium-metal batteries due to their compatibility with the lithium-metal negative electrode. Herein, cross-linked self-standing single-ion conducting polymer electrolytes are obtained via a facile UV-initiated radical polymerization using pentaerythritol tetraacrylate as the cross-linker and lithium (3-methacryloyloxypropylsulfonyl)-(trifluoromethylsulfonyl)imide as the ionic functional group. Incorporating propylene carbonate as charge-transport supporting additive allowed for achieving single-ion conductivities of 0.21 mS cm^{-1} at $20 \text{ }^\circ\text{C}$ and 0.40 mS cm^{-1} at $40 \text{ }^\circ\text{C}$, while maintaining a suitable electrochemical stability window for 4 V-class positive electrodes (cathodes). As a result, this single-ion polymer electrolyte featured good cycling stability and rate capability in $\text{Li}||\text{LiFePO}_4$ and $\text{Li}||\text{LiNi}_{0.6}\text{Mn}_{0.2}\text{Co}_{0.2}\text{O}_2$ cells. These results render this polymer electrolyte as potential alternative to liquid electrolytes for high-energy lithium-metal batteries.

promising candidates are lithium-metal batteries (LMBs),^[4,5] for which, however, safety remains an issue due to, e.g., the continuous electrolyte decomposition and dendrite growth upon lithium deposition.^[6,7] A widely followed approach to overcome these issues is the replacement of common liquid organic solvent-based electrolytes by solid electrolytes, promising the elimination of electrolyte leakage, lower flammability and greater thermal stability, enhanced interfacial stability, and suppression of dendritic lithium deposition.^[8–11] Compared with inorganic solid-state ionic conductors, polymer-based electrolytes are characterized by low densities (light weight), good flexibility, and facile processing; properties that are propitious for improving the energy density and facilitating the interfacial charge transfer, and reducing the cost.

1. Introduction

Rechargeable lithium-ion batteries (LIBs) are nowadays dominating the market of portable electronic devices and also increasing the transportation sector owing to their high energy and power density as well as their long-term stable operation.^[1–3] To further increase the driving range of electric vehicles, however, batteries with even higher energy densities are needed. Among the most


Great progress has been achieved since the pioneering work by Wright and co-workers as well as Armand and co-workers on poly(ethylene oxide) (PEO)-based electrolyte systems.^[12–14] In such “classic” polymer electrolytes, a lithium salt is dissolved into the polymer taking advantage of the strong coordination of the Li^+ cations and the ether oxygen of the polymer. Thus, the Li^+ transport is associated to the segmental relaxation of the polymer chains while the counter-anion moves freely in the empty space.^[15] This dual-ion conductivity suffers an uneven contribution of the two ionic species, i.e., the anion and cation. Additionally, it leads to the occurrence of charge concentration gradients and cell polarization, which jeopardizes the long-term cycling performance.^[16,17] These obstacles can be circumvented by covalently tethering the anionic function to the polymer, thus, realizing single-ion conducting polymer electrolytes (SIPes). Here, only the Li^+ cations are (theoretically) mobile—or in other words, for which the Li^+ transference number (t_{Li^+}) approaches unity, which is beneficial for achieving higher energy and power densities.^[16–19] To date, extensive efforts have been made to increase the ionic conductivity of SIPes. These include the design of weakly coordinating polyanionic functions with extensive negative charge delocalization, for instance, by introducing strong electron-withdrawing groups or elegantly modifying the anionic centers by coupling Li^+ with different heteroatoms to facilitate Li^+ conduction.^[20,21] Alternatively, SIPes are designed as self-assembling block copolymers with well-defined ionophilic domains that serve as Li^+ conduction pathways supported by “molecular transporters,” thus, yielding

H.-P. Liang, Z. Chen, X. Dong, T. Zinkevich, S. Indris, S. Passerini, D. Bresser

Helmholtz Institute Ulm (HIU)
 Helmholtzstrasse 11, Ulm 89081, Germany
 E-mail: stefano.passerini@kit.edu; dominic.bresser@kit.edu

H.-P. Liang, Z. Chen, X. Dong, S. Passerini, D. Bresser
 Karlsruhe Institute of Technology (KIT)
 P.O. Box 3640, Karlsruhe 76021, Germany

T. Zinkevich, S. Indris
 Institute for Applied Materials – Energy Storage Systems (IAM-ESS)
 Karlsruhe Institute of Technology (KIT)
 Hermann-von-Helmholtz-Platz 1,
 Eggenstein-Leopoldshafen 76344, Germany

 The ORCID identification number(s) for the author(s) of this article can be found under <https://doi.org/10.1002/marc.202100820>

© 2022 The Authors. *Macromolecular Rapid Communications* published by Wiley-VCH GmbH. This is an open access article under the terms of the Creative Commons Attribution License, which permits use, distribution and reproduction in any medium, provided the original work is properly cited.

DOI: 10.1002/marc.202100820

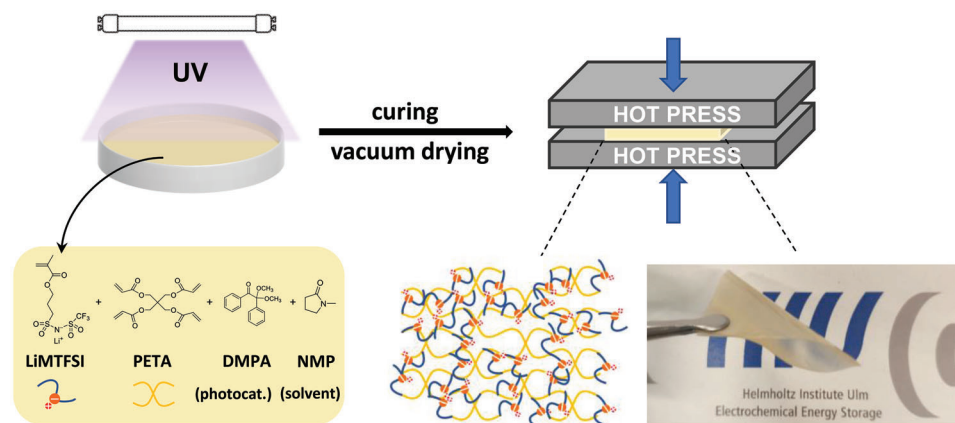


Figure 1. Schematic illustration of the UV-induced polymer synthesis including the precursors, the subsequent hot pressing, a scheme of the network-like product, and a photograph of the resulting polymer membrane.

remarkable ionic conductivities approaching $10^{-3} \text{ S cm}^{-1}$ even at ambient temperatures.^[22–24] Another approach targets the decrease of the glass transition temperature (T_g) in order to expedite the segmental motion of the polymer—similar to the majority of approaches followed for PEO-type electrolytes. This can be achieved, for instance, by chemical cross-linking, mitigating inter/intramolecular packing and by suppressing the local ordering.^[25,26] Simultaneously the knitted networks provide enhanced dimensional rigidity,^[27,28] which is beneficial for alleviating dendrite growth owing to a more homogeneous lithium deposition.^[29–35] One issue that commonly remains, however, is the electrochemical stability of the polymer toward oxidation. In fact, most polymer electrolytes show an anodic stability on metal electrodes (e.g., Ni, Pt, and Au) of up to 4.5 V versus Li^+/Li and sometimes even more, but cell tests are eventually limited to LiFePO_4 (LFP) cathodes^[36–38] and stable cycling with 4 V cathodes such as $\text{LiNi}_x\text{Mn}_y\text{Co}_{1-x-y}\text{O}_2$ (NMC), $\text{LiNi}_x\text{Co}_y\text{Al}_{1-x-y}\text{O}_2$ (NCA), or LiCoO_2 (LCO) remains an issue.^[22–24,39,40]

Herein, we present the facile synthesis of a new photo-cross-linked SIPE (PSIPE) for lithium-metal batteries, using pentaerythritol tetraacrylate (PETA) and lithium (3-methacryloyloxypropylsulfonyl)-(trifluoromethylsulfonyl)imide (LiMTFSI) as the building blocks. The cross-linked structure provides mechanical stability, while the flexible pendant chains retain segmental mobility. A smooth polymer electrolyte with an easily adjustable thickness was achieved by hot-pressing—a technique that has been well established for PEO-based electrolytes,^[41–44] but has not been reported so far for single-ion conductors based on other polymers—to the best of our knowledge. The incorporation of propylene carbonate (PC) into the PSIPE results in high ionic conductivity, excellent stability against metallic lithium, and, most remarkably, it enables excellent cycling stability of $\text{Li}|\text{LiFP}$ and $\text{Li}|\text{LiNi}_{0.6}\text{Mn}_{0.2}\text{Co}_{0.2}\text{O}_2$ (NMC₆₂₂) cells.

2. Results and Discussion

The synthesis via UV-induced photo-crosslinking and preparation of self-standing PSIPE membranes are depicted in **Figure 1** and described in detail in Figures S1–S3, Supporting Information. The LiMTFSI pendant ionic function was chosen owing to

its pronounced structural flexibility and the weak coordinating anion.^[45] A molar ratio of LiMTFSI to PETA of 2:1 was selected as such ratio yields polymer electrolyte membranes with both high ionic conductivity and suitable mechanical properties. An increased ratio of 3:1 leads to membranes that are simply too brittle for facile processing and handling, while a lower ratio (1:1) results in polymer electrolyte membranes with a significantly lower ionic conductivity, as will be discussed later on. Generally, the PSIPE as a whole provides many carbonyl- and ether-type functions, which are anticipated to facilitate charge transport by serving as additional coordination sites. The hot-pressing step allowed for carefully adjusting the thickness of the flexible membranes, characterized by a smooth surface (Figure S4, Supporting Information).

The analysis via Fourier-transform infrared (FT-IR) spectroscopy revealed the successful polymerization of the two building blocks LiMTFSI and PETA (**Figure 2a**). The stretching vibration band of the C = C double bond at $\tilde{\nu} = 1635\text{--}1618 \text{ cm}^{-1}$ vanished (see also the magnification in Figure S5, Supporting Information).^[46,47] The band ascribed to C = O ($\tilde{\nu} = 1734 \text{ cm}^{-1}$) is shifted toward higher wavenumbers for the PSIPE compared to LiMTFSI and PETA owing to the absence of the neighboring double bond. The absorption bands at 1320, 1118, and 1052 cm^{-1} are assigned to S = O as part of the sulfonylimide moieties. The band at $\tilde{\nu} = 1171 \text{ cm}^{-1}$ is assigned to the C–F bond of $-\text{CF}_3$ end group. The band at $\tilde{\nu} = 1265 \text{ cm}^{-1}$ corresponds to the C–O bond present in the ethoxylated moieties. The stretching vibration bands in the range from $\tilde{\nu} = 2960\text{--}2880 \text{ cm}^{-1}$ are ascribed to the $-\text{CH}_2-$ linkages and $-\text{CH}_3$.

The thermal stability of the PSIPE was studied by thermogravimetric analysis (TGA) in a mixture of N_2/O_2 (V:V = 50:50) (Figure S6, Supporting Information). The onset of the thermal decomposition is around $165 \text{ }^\circ\text{C}$, which is suitable for the common processing (e.g., extrusion, hot pressing, and drying) procedures during battery cell fabrication. Differential scanning calorimetry (DSC, Figure 2b) revealed a T_g of $-29 \text{ }^\circ\text{C}$, which is significantly lower than the values that have been reported for other crosslinked SIPEs.^[37,35] This finding is ascribed to the highly flexible pendant ionic groups. Also important to note is that only one T_g was detected, corroborating a homogeneous distribution of the two building blocks LiMTFSI and PETA in the PSIPE.^[48]

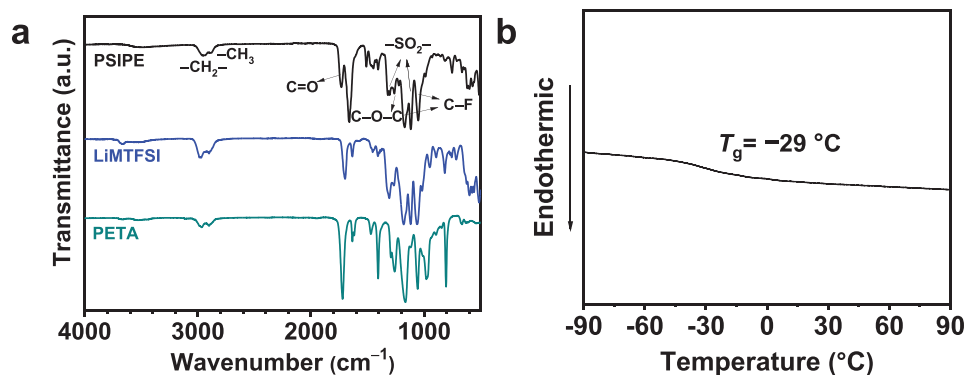


Figure 2. a) FT-IR spectra of the PC-free PSIPE and the two building blocks. b) DSC data of the PC-free PSIPE with an indication of the T_g .

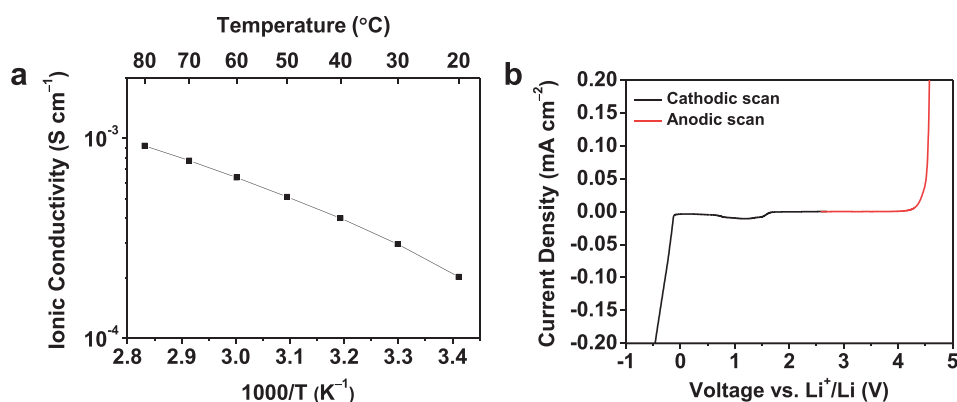


Figure 3. a) Plot of the ionic conductivity as a function of temperature for the PC-containing PSIPE and b) the electrochemical stability window as determined by linear sweep voltammetry at 40 °C.

For the subsequent electrochemical characterization, PC was incorporated into the PSIPE to favor the Li^+ -ion mobility. Upon optimization, 80 wt% PC (the wt% refers to the mass of the dry polymer membrane) was selected as the best composition with regard to the mechanical properties and ionic conductivity of the polymer electrolyte. Both the PC-free and the swollen membrane provide a suitable flexibility and appropriate mechanical properties for the use in laboratory-scale battery cells, as demonstrated in Video S1 (Supporting Information). The plot of the ionic conductivity is presented in **Figure 3a**. The nonlinear increase in conductivity with temperature indicates Vogel-Tammann-Fulcher (VTF) behavior, implying that Li^+ ions are (at least partially) coupled to the segmental motion of the PSIPE, potentially supported by the PC molecules. The ionic conductivity at 20 °C is 0.21 mS cm^{-1} and increases to 0.40 mS cm^{-1} at 40 °C, which is substantially higher than for the 1:1 LiMTFSI:PETA ratio, for which it is 0.12 and 0.27 mS cm^{-1} at 20 and 40 °C, respectively (not shown herein). This is also higher than most of the recently reported SIPEs (Table S1, Supporting Information), which is attributed to the combination of a rather low T_g , the highly delocalized negative charge at the anionic group, as well as the plasticizing effect and provision of additional coordination sites by the PC molecules. As a matter of fact, the conductivity at 40 °C is considered to be sufficient for use in electric vehicles when the transference number approaches unity.^[19] Another

important parameter determining the charge transport kinetics is the limiting current density, which was determined via linear sweep voltammetry (LSV) yielding 0.68 mA cm^{-2} at 40 °C (Figure S7, Supporting Information). Additional LSV experiments were performed to evaluate the electrochemical stability (Figure 3b). The sharp increase in current density exceeding 0.02 mA cm^{-2} during the anodic sweep beyond 4.4 V indicates the onset of the oxidative decomposition. Upon the cathodic sweep, a broad peak is observed in the range from 1.0 to 1.6 V, which is assigned to the reductive decomposition of PC and the electrochemical reduction of the native oxide layer on the nickel electrode.^[49,50] Below 0 V the current rapidly increases owing to the plating of metallic lithium on the working electrode.

To further evaluate the stability toward metallic lithium, we conducted extended lithium stripping and plating experiments at varying current densities in symmetric Li||Li cells (**Figure 4**). As shown in Figure 4a, when applying a low current density of 0.01 mA cm^{-2} , the overpotential is as low as 6 mV. For elevated applied current densities of 0.10 and 0.20 mA cm^{-2} , the overpotential increases to 0.054 and 0.12 V, respectively. These values are half of those reported for the single-ion conducting polymer electrolyte comprising boron-centered anions and organic carbonates as plasticizer^[51] or the poly(ionic liquid)/ Al_2O_3 composite electrolyte comprising a highly concentrated ionic liquid.^[52] When decreasing the current density eventually back

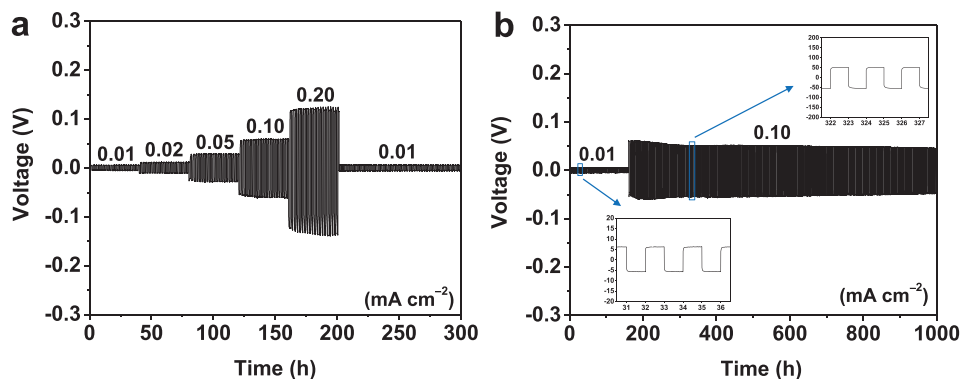


Figure 4. Lithium stripping/plating tests in symmetric Li||Li cells at 40 °C employing PSiPE as the electrolyte and separator. a) A symmetric cell subjected to varying current densities; each stripping/plating step lasts for 1 h. b) Long-term Li stripping/plating test at 0.01 mA cm⁻² for the initial 80 cycles and 0.10 mA cm⁻² for the subsequent cycles; insets: magnification of the corresponding voltage profiles at both current densities applied.

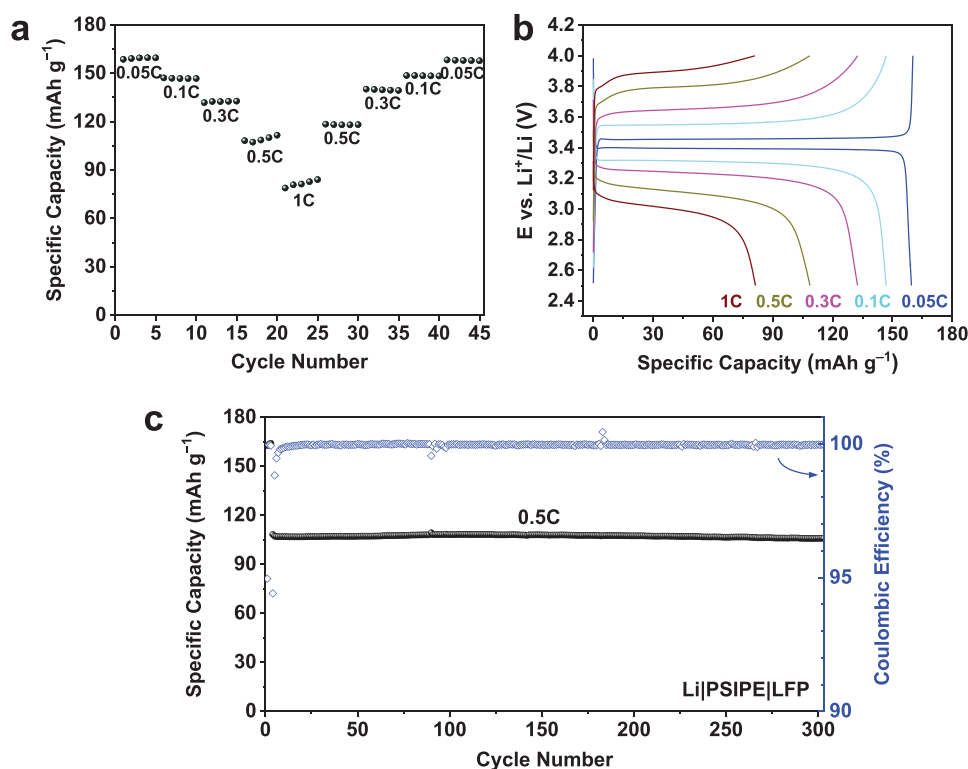


Figure 5. Galvanostatic cycling of Li|PSiPE|LFP cells at 40 °C within a voltage range of 2.5–4.0 V: a) Evaluation of the discharge capacity at varying dis-/charge rates; b) The corresponding voltage profiles for selected cycles at the different dis-/charge rates; c) The long-term galvanostatic cycling at 0.5 C after three formation cycles at 0.05 C.

to 0.01 mA cm⁻², the overpotential decreases to the initial value, indicating a very stable Li|electrolyte interface. This finding is further corroborated by the long-term stripping/plating experiment presented in Figure 4b. The overpotential does not increase even after 1000 h of continuous cycling and remains very stable—even slightly decreasing, which might be related to an increasing Li|electrolyte interface as a result of the stripping and plating. The magnification of the voltage response provided as insets show that the voltage is essentially constant, which confirms that there is no detectable concentration gradient evolving.

The suitability of this PSiPE to serve as electrolytes in lithium-metal batteries was subsequently studied in Li|PSiPE|LFP cells, setting the cut-off voltages to 2.5 and 4.0 V (Figure 5). As displayed in Figure 5a, the cells provide a reversible capacity of 159, 147, 132, 109, and 81 mAh g⁻¹ at dis-/charge rates of 0.05 C, 0.1 C, 0.3 C, 0.5 C, and 1 C, respectively. This decrease originates from a significant increase in polarization (Figure 5b). The subsequent decrease of the C rate, however, reveals that the capacity is well recovered and there is no apparent fading (Figure 5a). In fact, when applying a constant dis-/charge rate of 0.5 C for 300 cycles

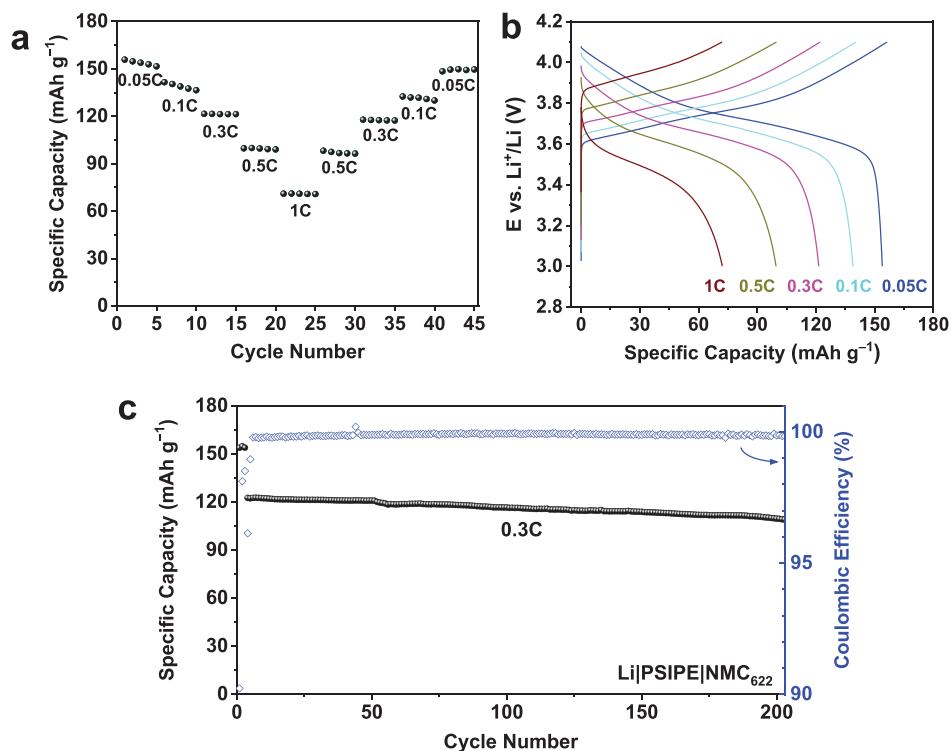


Figure 6. Galvanostatic cycling of Li|PSIPE|NMC₆₂₂ cells at 40 °C within a voltage range of 3.0–4.1 V: a) Evaluation of the discharge capacity at varying dis-/charge rates; b) the corresponding voltage profiles for selected cycles at the different dis-/charge rates; c) the long-term galvanostatic cycling at 0.3 C after three formation cycles at 0.05 C.

(Figure 5c), owing to the high average Coulombic efficiency of 99.9%, the reversible capacity decreased by only 2 mAh g⁻¹, i.e., from 108 to 106 mAh g⁻¹, corresponding to an excellent capacity retention of 98.1%—a value that is among the highest reported for SIPEs in Li||LFP cells (Table S1, Supporting Information).

In a next step, Li|PSIPE|NMC₆₂₂ cells were assembled to evaluate the compatibility of the polymer electrolyte with high-energy Ni-rich cathode materials. Initially, the cut-off voltages were set to 3.0 and 4.1 V, i.e., the upper one slightly higher than for LFP-based cells. The results are shown in Figure 6. The cells delivered reversible specific capacities of about 154 mAh g⁻¹ at 0.05 C, 139 mAh g⁻¹ at 0.1 C, 121 mAh g⁻¹ at 0.3 C, 100 mAh g⁻¹ at 0.5 C, and 72 mAh g⁻¹ at 1 C (Figure 6a) and also in this case a significant polarization is observed when increasing the dis-/charge rate (Figure 6b), while the capacity is well recovered when decreasing the C rate again (Figure 6a). In fact, when applying a constant dis-/charge rate of 0.3 C, the capacity remains very stable for more than 200 cycles with an initial reversible capacity of ≈123 mAh g⁻¹ at 0.3 C and about 110 mAh g⁻¹ after 200 cycles (i.e., a capacity retention of 89.4%), accompanied by an average Coulombic efficiency of 99.8% (Figure 6c). When increasing the upper cut-off voltage to 4.2 V (Figure S8, Supporting Information), however, the capacity retention decreases and the initial Coulombic efficiency also decreases from 90.2% (as in the case of 4.1 V) to 85.1%. While the interface might be stabilized by, for instance, applying suitable inorganic or organic surface coatings on the cathode active material particles,^[53,54] this finding nicely highlights the need for evaluating the suitability of (polymer) electrolytes in real cells rather than only

by determining the electrochemical stability window in, e.g., Li||Ni cells.^[55,56]

3. Conclusions

The photo-crosslinked single-ion conducting polymer electrolyte (PSIPE), synthesized via a facile radical polymerization, provides self-standing membranes that show high ionic conductivities of 0.21 mS cm⁻¹ at 20 °C and 0.40 mS cm⁻¹ at 40 °C. Moreover, this polymer electrolyte shows an excellent stability toward lithium metal, as confirmed by an essentially constant overpotential when continuously stripping and plating lithium in symmetric Li||Li cells for 1000 h. The high electrochemical stability toward oxidation also allows for the very stable cycling of Li||LFP and Li||NMC₆₂₂ cells for several hundred cycles when limiting the upper cut-off voltage to 4.1 V in the latter case. These results render the PSIPE a suitable candidate for 4 V lithium-metal batteries.

Supporting Information

Supporting Information is available from the Wiley Online Library or from the author.

Acknowledgements

The authors would like to acknowledge financial support from the Federal Ministry of Education and Research (BMBF) within the FestBatt project (03XP0175B) and from the Helmholtz Association.

Open Access funding enabled and organized by Projekt DEAL.

Conflict of Interest

The authors declare no conflict of interest.

Data Availability Statement

Research data are not shared.

Keywords

batteries, lithium, polymer electrolytes, single-ion conductors, UV cross-linking

Received: November 28, 2021

Revised: January 6, 2022

Published online:

- [1] M. Marinaro, D. Bresser, E. Beyer, P. Faguy, K. Hosoi, H. Li, J. Sakovica, K. Amine, M. Wohlfahrt-Mehrens, S. Passerini, *J. Power Sources* **2020**, 459, 228073.
- [2] D. Bresser, K. Hosoi, D. Howell, H. Li, H. Zeisel, K. Amine, S. Passerini, *J. Power Sources* **2018**, 382, 176.
- [3] M. Armand, P. Axmann, D. Bresser, M. Copley, K. Edström, C. Ekberg, D. Guyomard, B. Lestriez, P. Novák, M. Petranikova, W. Porcher, S. Trabesinger, M. Wohlfahrt-Mehrens, H. Zhang, *J. Power Sources* **2020**, 479, 228708.
- [4] X.-B. Cheng, R. Zhang, C.-Z. Zhao, Q. Zhang, *Chem. Rev.* **2017**, 117, 10403.
- [5] A. Varzi, K. Thanner, R. Scipioni, D. Di Lecce, J. Hassoun, S. Dörfler, H. Altheus, S. Kaskel, C. Prehal, S. A. Freunberger, *J. Power Sources* **2020**, 480, 228803.
- [6] B. Horstmann, J. Shi, R. Amine, M. Werres, X. He, H. Jia, F. Hausen, I. Cekic-Laskovic, S. Wiemers-Meyer, J. Lopez, D. Galvez-Aranda, F. Baakes, D. Bresser, C.-C. Su, Y. Xu, W. Xu, P. Jakes, R.-A. Eichel, E. Figgemeier, U. Krewer, J. M. Seminario, P. B. Balbuena, C. Wang, S. Passerini, Y. Shao-Horn, M. Winter, K. Amine, R. Kostecki, A. Latz, *Energy Environ. Sci.* **2021**, 14, 5289.
- [7] X. He, D. Bresser, S. Passerini, F. Baakes, U. Krewer, J. Lopez, C. T. Mallia, Y. Shao-Horn, I. Cekic-Laskovic, S. Wiemers-Meyer, F. A. Soto, V. Ponce, J. M. Seminario, P. B. Balbuena, H. Jia, W. Xu, Y. Xu, C. Wang, B. Horstmann, R. Amine, C.-C. Su, J. Shi, K. Amine, M. Winter, A. Latz, R. Kostecki, *Nat. Rev. Mater.* **2021**, 6, 1036.
- [8] J. Kalhoff, G. G. Eshetu, D. Bresser, S. Passerini, *ChemSusChem* **2015**, 8, 2154.
- [9] A. Mauger, M. Armand, C. M. Julien, K. Zaghib, *J. Power Sources* **2017**, 353, 333.
- [10] Y. Zheng, Y. Yao, J. Ou, M. Li, D. Luo, H. Dou, Z. Li, K. Amine, A. Yu, Z. Chen, *Chem. Soc. Rev.* **2020**, 49, 8790.
- [11] D.-S. Kwon, H. J. Kim, J. Shim, *Macromol. Rapid Commun.* **2021**, 42, 2100279.
- [12] D. Zhou, D. Shanmukaraj, A. Tkacheva, M. Armand, G. Wang, *Chem* **2019**, 5, 2326.
- [13] D. E. Fenton, J. M. Parker, P. V. Wright, *Polymer* **1973**, 14, 589.
- [14] M. Armand, *Solid State Ionics* **1983**, 9–10, 745.
- [15] D. Bresser, S. Lyonnard, C. Iojoiu, L. Picard, S. Passerini, *Mol. Syst. Des. Eng.* **2019**, 4, 779.
- [16] M. Doyle, T. F. Fuller, J. Newman, *Electrochim. Acta* **1994**, 39, 2073.
- [17] K. E. Thomas, S. E. Sloop, J. B. Kerr, J. Newman, *J. Power Sources* **2000**, 89, 132.
- [18] H. Zhang, C. Li, M. Piszcz, E. Coya, T. Rojo, L. M. Rodriguez-Martinez, M. Armand, Z. Zhou, *Chem. Soc. Rev.* **2017**, 46, 797.
- [19] H.-K. Kim, V. Srinivasan, *J. Electrochem. Soc.* **2020**, 167, 130520.
- [20] Q. Ma, H. Zhang, C. Zhou, L. Zheng, P. Cheng, J. Nie, W. Feng, Y.-S. Hu, H. Li, X. Huang, L. Chen, M. Armand, Z. Zhou, *Angew. Chem., Int. Ed.* **2016**, 55, 2521.
- [21] K. Deng, Q. Zeng, D. Wang, Z. Liu, Z. Qiu, Y. Zhang, M. Xiao, Y. Meng, *J. Mater. Chem. A* **2020**, 8, 1557.
- [22] H.-D. Nguyen, G.-T. Kim, J. Shi, E. Paillard, P. Judeinstein, S. Lyonnard, D. Bresser, C. Iojoiu, *Energy Environ. Sci.* **2018**, 11, 3298.
- [23] Z. Chen, D. Steinle, H.-D. Nguyen, J.-K. Kim, A. Mayer, J. Shi, E. Paillard, C. Iojoiu, S. Passerini, D. Bresser, *Nano Energy* **2020**, 77, 105129.
- [24] D. Steinle, Z. Chen, H.-D. Nguyen, M. Kuenzel, C. Iojoiu, S. Passerini, D. Bresser, *J. Solid State Electrochem.* **2021**, 26, 97.
- [25] H. Stutz, K.-H. Illers, J. Mertes, *J. Polym. Sci. Part B Polym. Phys.* **1990**, 28, 1483.
- [26] J. Stejny, *Polym. Bull.* **1996**, 36, 617.
- [27] S.-J. Kwon, D.-G. Kim, J. Shim, J. H. Lee, J.-H. Baik, J.-C. Lee, *Polymer* **2014**, 55, 2799.
- [28] G. Homann, L. Stolz, K. Neuhaus, M. Winter, J. Kasnatscheew, *Adv. Funct. Mater.* **2020**, 30, 2006289.
- [29] M. D. Tikekar, L. A. Archer, D. L. Koch, *Sci. Adv.* **2016**, 2, e1600320.
- [30] S. Choudhury, R. Mangal, A. Agrawal, L. A. Archer, *Nat. Commun.* **2015**, 6, 10101.
- [31] H. Wu, Y. Cao, H. Su, C. Wang, *Angew. Chem., Int. Ed.* **2018**, 57, 1361.
- [32] R. Khurana, J. L. Schaefer, L. A. Archer, G. W. Coates, *J. Am. Chem. Soc.* **2014**, 136, 7395.
- [33] K. Dai, C. Ma, Y. Feng, L. Zhou, G. Kuang, Y. Zhang, Y. Lai, X. Cui, W. Wei, *J. Mater. Chem. A* **2019**, 7, 18547.
- [34] K. Deng, J. Qin, S. Wang, S. Ren, D. Han, M. Xiao, Y. Meng, *Small* **2018**, 14, 1801420.
- [35] J. Zhang, S. Wang, D. Han, M. Xiao, L. Sun, Y. Meng, *Energy Storage Mater.* **2020**, 24, 579.
- [36] H. Oh, K. Xu, H. D. Yoo, D. S. Kim, C. Chanthad, G. Yang, J. Jin, I. A. Ayhan, S. M. Oh, Q. Wang, *Chem. Mater.* **2016**, 28, 188.
- [37] Y. Zhong, L. Zhong, S. Wang, J. Qin, D. Han, S. Ren, M. Xiao, L. Sun, Y. Meng, *J. Mater. Chem. A* **2019**, 7, 24251.
- [38] C. Li, B. Qin, Y. Zhang, A. Varzi, S. Passerini, J. Wang, J. Dong, D. Zeng, Z. Liu, H. Cheng, *Adv. Energy Mater.* **2019**, 9, 1803422.
- [39] K. Borzutzki, J. Thienenkamp, M. Diehl, M. Winter, G. Bruncklaus, *J. Mater. Chem. A* **2019**, 7, 188.
- [40] K. Borzutzki, D. Dong, C. Wölke, M. Kruteva, A. Stellhorn, M. Winter, D. Bedrov, G. Bruncklaus, *iScience* **2020**, 23, 101417.
- [41] M. Wetjen, G.-T. Kim, M. Joost, G. B. Appetecchi, M. Winter, S. Passerini, *J. Power Sources* **2014**, 246, 846.
- [42] Z. Chen, G.-T. Kim, Z. Wang, D. Bresser, B. Qin, D. Geiger, U. Kaiser, X. Wang, Z. X. Shen, S. Passerini, *Nano Energy* **2019**, 64, 103986.
- [43] N. Angulakshmi, Y. Zhou, S. Suriyakumar, R. B. Dhanalakshmi, M. Satishrajan, S. Alwarappan, M. H. Alkordi, A. M. Stephan, *ACS Omega* **2020**, 5, 7885.
- [44] L. Porcarelli, P. Sutton, V. Bocharova, R. H. Aguirresarobe, H. Zhu, N. Goujon, J. R. Leiza, A. Sokolov, M. Forsyth, D. Mecerreyes, *ACS Appl. Mater. Interfaces* **2021**, 13, 54354.
- [45] L. Porcarelli, A. S. Shaplov, F. Bella, J. R. Nair, D. Mecerreyes, C. Gerbaldi, *ACS Energy Lett.* **2016**, 1, 678.
- [46] J. Zhu, Z. Zhang, S. Zhao, A. S. Westover, I. Belharouak, P.-F. Cao, *Adv. Energy Mater.* **2021**, 11, 2003836.
- [47] E.-H. Kil, K.-H. Choi, H.-J. Ha, S. Xu, J. A. Rogers, M. R. Kim, Y.-G. Lee, K. M. Kim, K. Y. Cho, S.-Y. Lee, *Adv. Mater.* **2013**, 25, 1395.
- [48] S. Choudhury, S. Stalin, D. Vu, A. Warren, Y. Deng, P. Biswal, L. A. Archer, *Nat. Commun.* **2019**, 10, 4398.
- [49] X. Zhang, R. Kostecki, T. J. Richardson, J. K. Pugh, P. N. Ross, *J. Electrochem. Soc.* **2001**, 148, A1341.
- [50] G. T. Kim, G. B. Appetecchi, M. Carewska, M. Joost, A. Balducci, M. Winter, S. Passerini, *J. Power Sources* **2010**, 195, 6130.

- [51] K. Liu, S. Jiang, T. L. Dzwiniel, H.-K. Kim, Z. Yu, N. L. Dietz Rago, J.-J. Kim, T. T. Fister, J. Yang, Q. Liu, J. Gilbert, L. Cheng, V. Srinivasan, Z. Zhang, C. Liao, *ACS Appl. Mater. Interfaces* **2020**, *12*, 29162.
- [52] G. M. A. Girard, X. Wang, R. Yunis, D. R. Macfarlane, A. J. Bhat-tacharyya, M. Forsyth, P. C. Howlett, *Batter. Supercaps* **2019**, *2*, 229.
- [53] J. Qiu, X. Liu, R. Chen, Q. Li, Y. Wang, P. Chen, L. Gan, S.-J. Lee, D. Nordlund, Y. Liu, X. Yu, X. Bai, H. Li, L. Chen, *Adv. Funct. Mater.* **2020**, *30*, 1909392.
- [54] Z. Chen, H.-D. Nguyen, M. Zarrabeitia, H.-P. Liang, D. Geiger, J.-K. Kim, U. Kaiser, S. Passerini, C. Iojoiu, D. Bresser, *Adv. Funct. Mater.* **2021**, *31*, 2105343.
- [55] K. Xu, S. P. Ding, T. R. Jow, *J. Electrochem. Soc.* **2019**, *146*, 4172.
- [56] A. Mathew, M. J. Lacey, D. Brandell, *J. Power Sources Adv.* **2021**, *11*, 100071.